AE-503 AEROELASTICITY

A compiled report of projects

Submitted by

Sudhi Sharma P.V

Contents

List of Figures

List of Tables

Chapter 1

Aeroelastic properties of a 2D airfoil

1.1 Noise properties Analysis

1.1.1 Using the 0RPM data, for which no pitch dynamics was excited, analysis the noise properties by calculating its variance, PSD and PDF.

Ans:

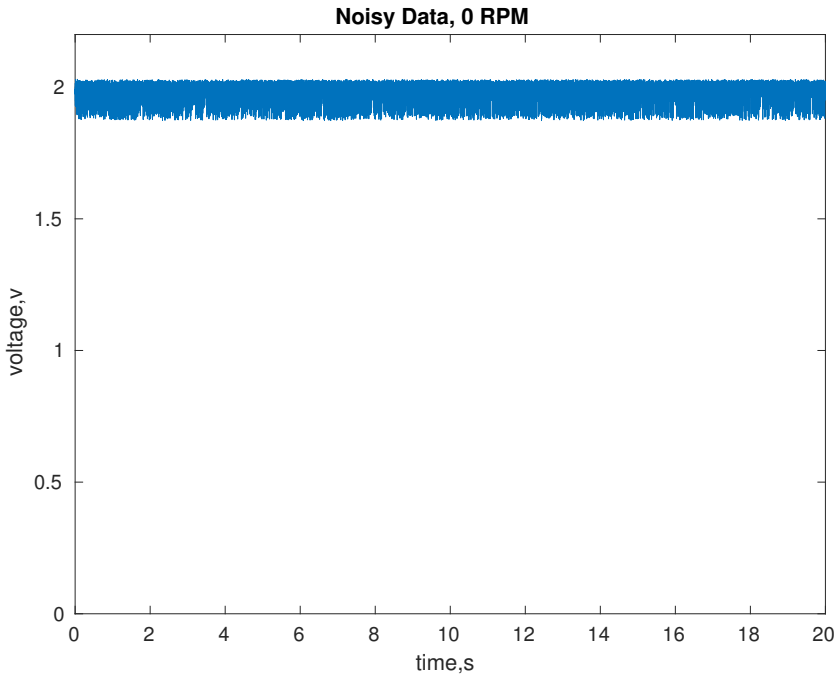

Figure 1.1: Noisy 0 RPM data

From the histogram plot in Fig.1.2 we can see that the noise data is spread across a wide range. It does not correspond to any particular distribution of data. By filtering out

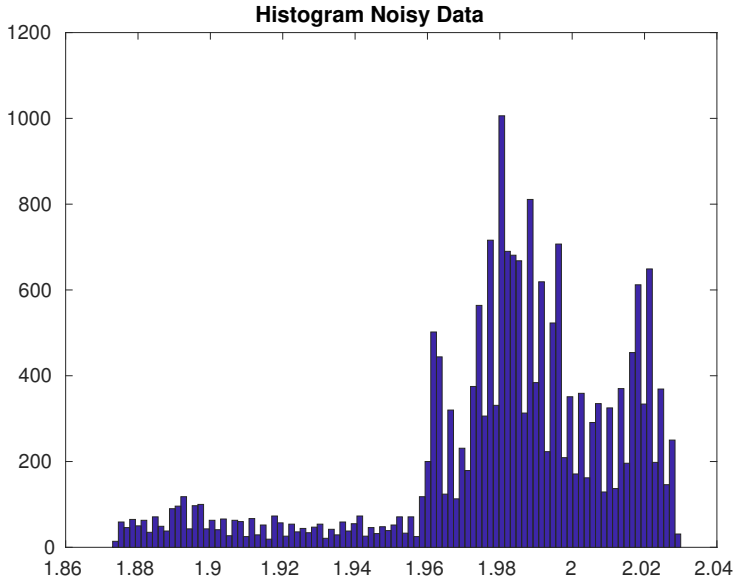

Figure 1.2: Histogram of noisy 0 RPM data

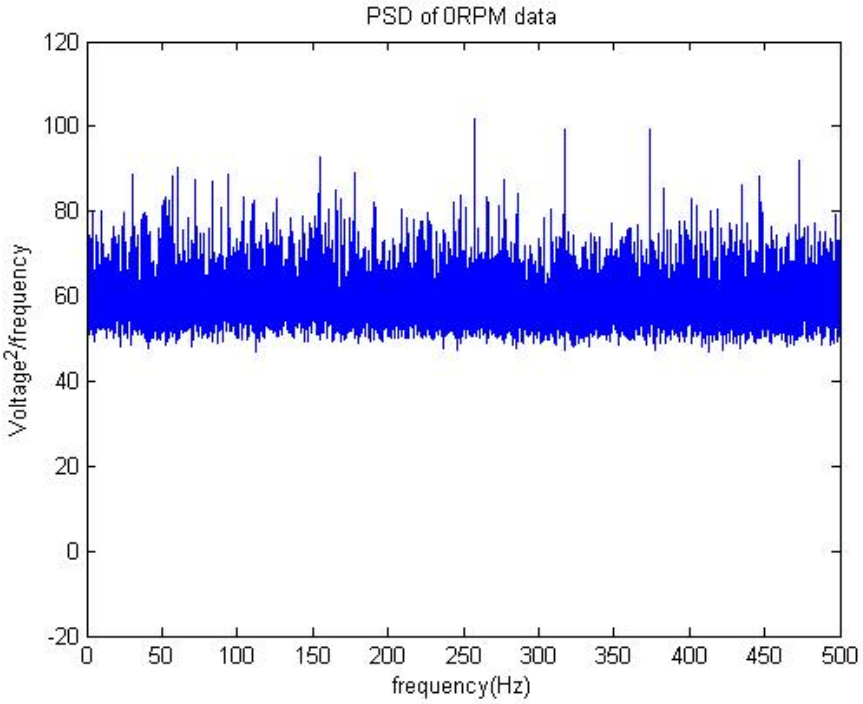

Figure 1.3: PSD of noisy 0 RPM data

the high frequency componets one will be able to understand the inherent distribution of the noise.

Mean, $\mu = 1.981$
Variance, $\sigma = 0.001$

From the PSD plot above, Fig.1.3, it is evident that all frequency components are participating equally in the noise. This corresponds to a white noise. Filtering out the high frequency from this data will allow us to understand the main contributing frequency range of noise. This will also allow us to seperate out this noise from the main signal data under consideration.

1.1.2 In a second analysis, filter out the high frequency content, and re-calculate variance, PSD and PDF. Numerical filter is provided.

A suitable FFT-Fast Fourier Transform filter is being used which removes the high frequency content from signal. A passband frequency of 30 Hz and stop band frequency of 35 Hz is being used in the filter. In Fig.1.4 the filtered 0 RPM data is plot overlapped with the noisy signal showing the smoothness and accuracy of the filtered data.

Mean, $\mu = 1.981$
Variance, $\sigma = 0.00007$

$$f(x|\mu,\sigma) = \frac{1}{\sqrt{2\pi\sigma^2}} e^{-\frac{(x-\mu)^2}{2\sigma^2}} \tag{1.1}$$

From the PSD in Fig.1.6 one can ensure that all the frequencies from 0-35 are included and that all higher frequencies are cut down. PDF of filtered signal is overlapped with the Gaussian distribution (Eq.1.1) with the same mean and variance as of signal(Fig.1.5). It can be seen that the signal filtered closely matches the normal distribution and thus the mean value of this data can be taken as representative of the whole noisy data.

1.1.3 Using a case with airspeed and focusing on a region without any aeroelastic oscillations, re-calculate the noise variance, PSD and PDF.

In order to understand the behaviour of the noise within a data with flow, a section of signal from 10 s to 20 s has been cut out from a 100 RPM data.

Mean, $\mu = 1.973$
Variance, $\sigma = 0.00006$

Mean of the signal is found to vary from the previous 0 RPM data. This may be because of the disturbances after the wing movement during experiment. PDF of the noise could be matched again with a Gaussian distribution with same mean and variance. Also, the PSD of noise doesn't show any significant difference from previous data.

From the noise properties analysis, it can be inferred that the noise varies around a mean value of 1.981 volts. The significant part of the noise lies in the range from 0-35 Hz.

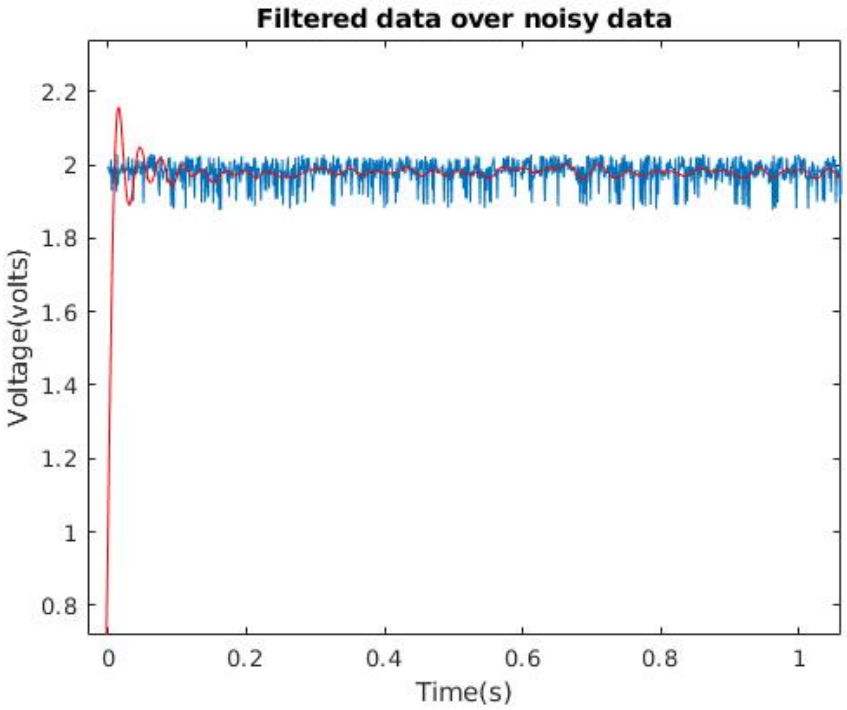

Figure 1.4: Filtered data, 0 RPM

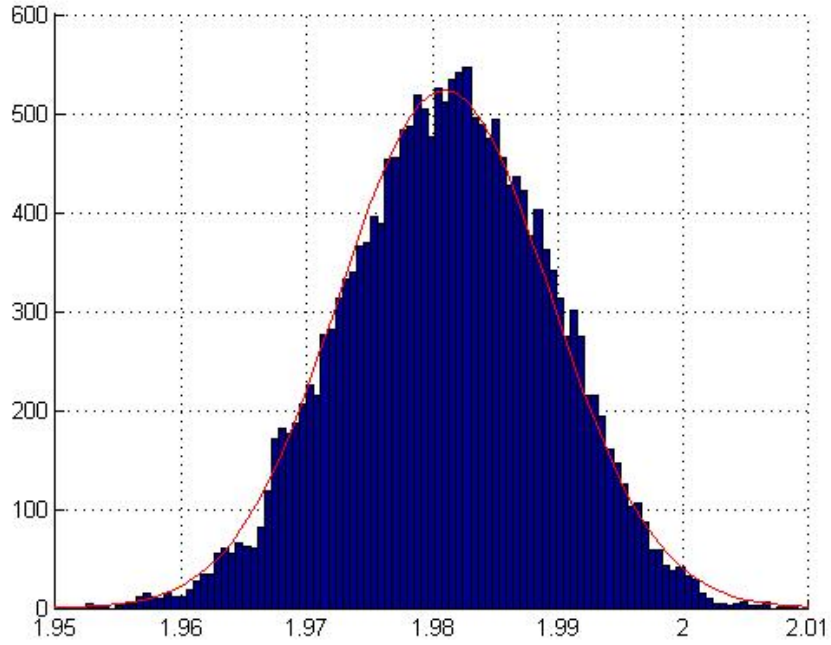

Figure 1.5: Histogram of Filtered data with Gaussian Distribution

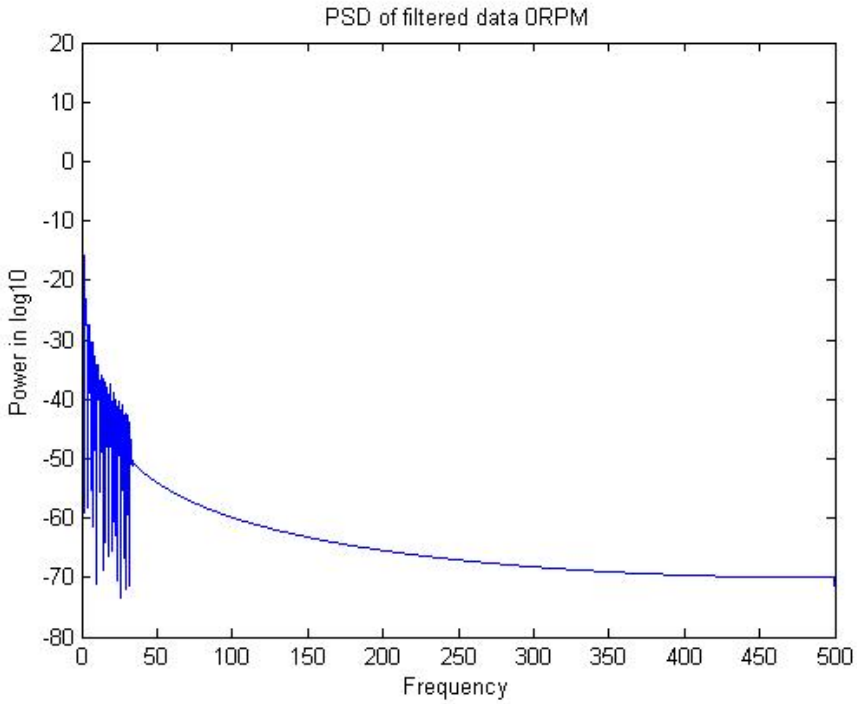

Figure 1.6: Filtered data, 0 RPM

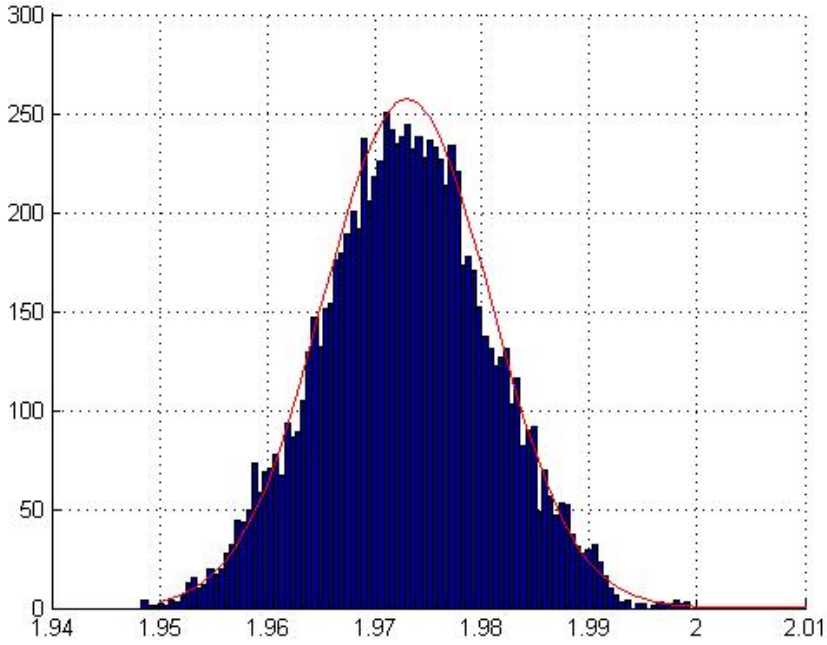

Figure 1.7: Histogram of Filtered data with Gaussian Distribution taken at 100 RPM without oscillations

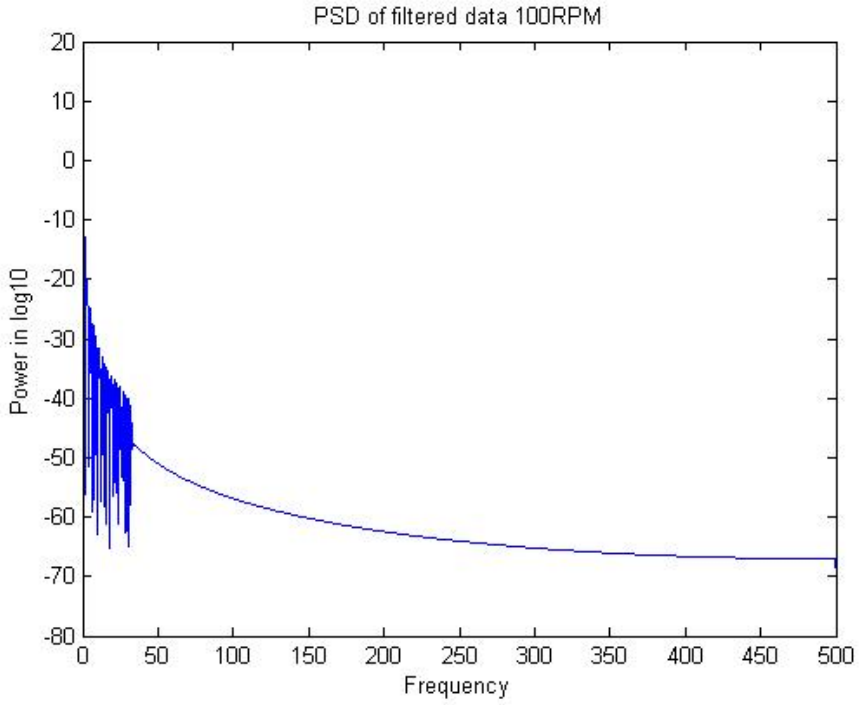

Figure 1.8: PSD of Filtered data taken at 100 RPM without oscillations

1.2 Aeroelastic Analysis

1.2.1 For the no-flow case, using the experimental data (FreeDecay1) and the logarithmic decrement method, calculate the stiffness coefficient, Ks, and the viscous damping coefficient, Ds, in order to obtain the following equation of motion, $I_{EA}\ddot{\theta} + D_s\dot{\theta} + K_s\theta = 0$. Before analyzing the data, you will need to filter out the (measurement) noise from the time response.

To perform the aeroelastic analysis of the data, one need to remove the noise from the signal. After removing the noise, it has to be converted to degree units from voltage using the degree-volt slope value. It has to be noted that the FFT operation performed might introduce some artificial content in the signal and might effect the properties of the signal. Therefore, the filtered signal has been taken cut at 0.2 s to 20 s and this part is considered for further analysis.

The degree-volt calibration slope value has been given to be -16.808 degree/volt. The equation for degree has been derived from this as below and the signal is converted to degrees.

$$degree = 33.296 - (volts * 16.808) \tag{1.2}$$

By varying the passband and stopband frequency and looking at the PSD data, Fig.1.9 one can see clearly that the free decay signal has a frequency in between 3 and 5 Hz. One should also ensure that the signal is smooth harmonic and gives exact peaks.

A frequency range of 3-5 Hz has been used as passband and stopband frequency. This provides us with a smooth harmonic signal(Fig.1.10) on which the logarithmic decrement

method can be applied.

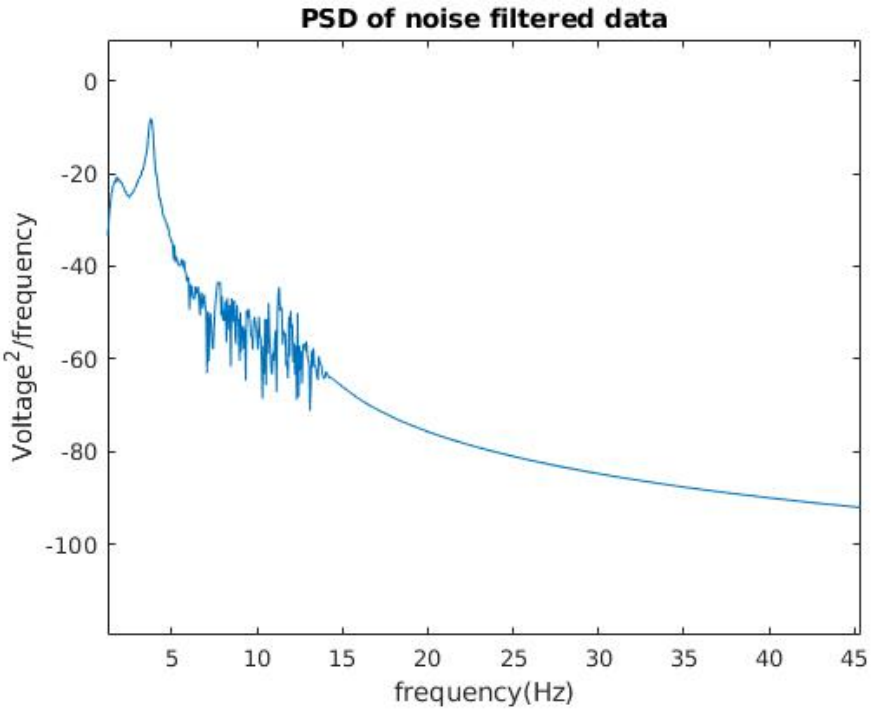

Figure 1.9: PSD of Free Decay data Filtered at 10-15 Hz

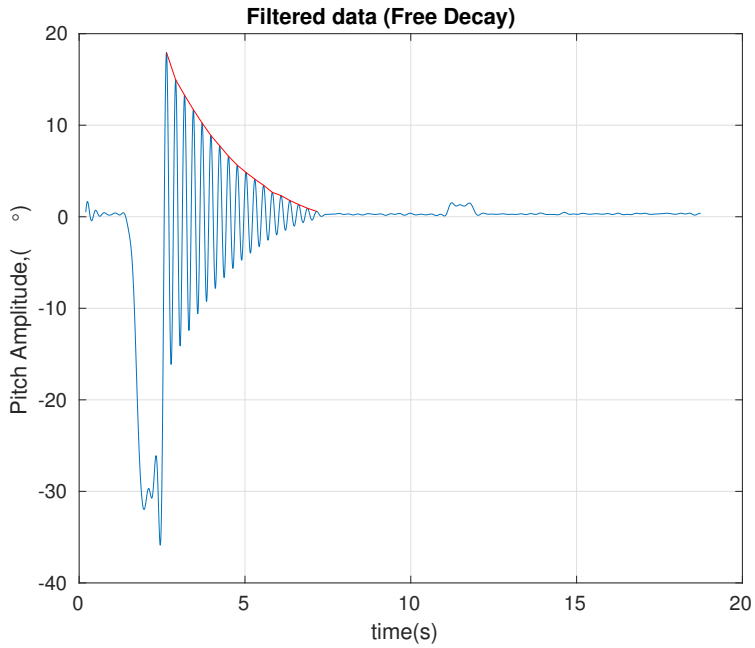

Figure 1.10: Filtered Free Decay Data

The free vibration equation for a system with a natural frequency ω_n and damping ratio ξ can be written as in Eq.1.3. General solution to this homogenous second order ODE

can be found as Eq.1.4.

$$\ddot{x} + 2\xi\omega_n\dot{x} + {\omega_n}^2 x = 0 \tag{1.3}$$

$$x = Ae^{-\xi\omega_n t}(\cos\omega_d t - \phi) \tag{1.4}$$

Logarithmic decrement, Δ is defined as the natural log of ratio of peaks/amplitudes of the harmonic solution (Eq.1.5).

$$\Delta = ln(\frac{x_1}{x_2}) \tag{1.5}$$

Substituting x_1 and x_2 found from the general solution in Eq.1.4 in to Eq.1.5 gives us the expression for damping ratio, ξ in terms of Δ as

$$\xi = \frac{\Delta}{\sqrt{4\pi^2 + \Delta^2}} \tag{1.6}$$

Selecting the right peak from the signal is one of the most sensitive tasks here. For cases of wing under flow, it is quite possible to have non-linearities due to stall effect at high pitch amplitudes and Reynolds number effect in low pitch amplitudes. Selecting a peak in any of these regions might cause the damping ration to be wrong and thus the whole analysis. For accurate results one must pick the damping ratio value in the linear regime of flow.

In order to understand in detail about the linear regime and the selection of damping ratio, more information about variation of damping ratio and damped frequency with respect to time as well as pitch amplitude has to be known. Looking at these graphs and finding out the non-linear regimes in the plot would give an idea about the linear regimes.

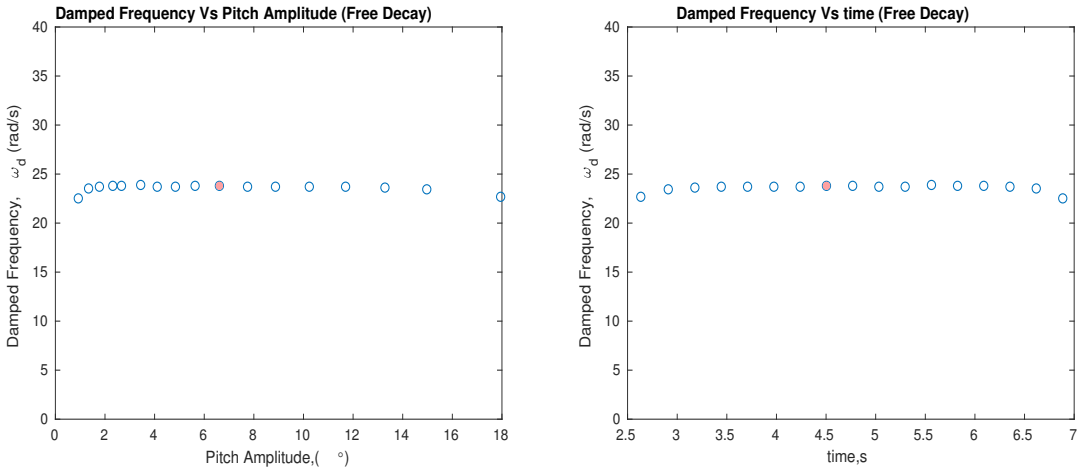

(a) Pitch Amplitude (b) Time

Figure 1.11: Variation of Damped frequency

Damping ratio ξ found from the above graphs can be used to find the damping coefficient D_s and stiffness coefficient K_s from Eq.1.3. The free vibration values of the wing are found to be as below,

Damping ratio, $\xi = 2.5\%$
Damped Frequency, $\omega_d = 23.80\ rad/s$
Natural Frequency, $\omega_n = 23.81\ rad/s$

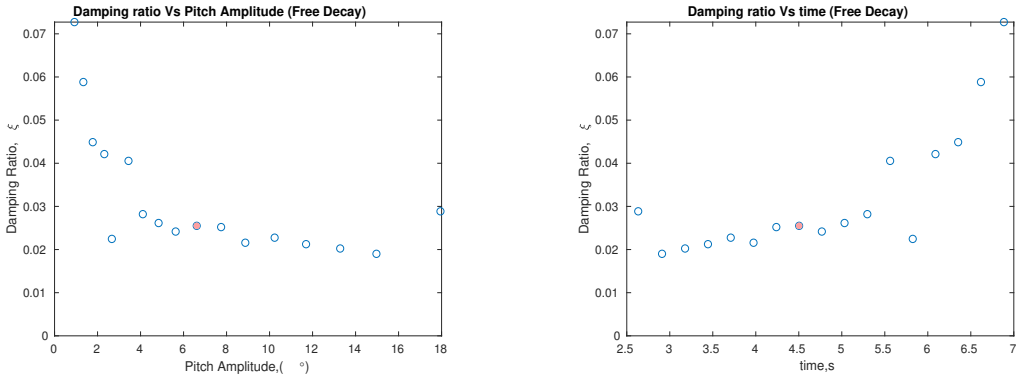

(a) Pitch Amplitude (b) Time

Figure 1.12: Variation of Damping Ratio

Damping Coefficient, $D_s = 0.0013\ Nm\ rad/s$
Stiffness Coefficient, $K_s = 0.624\ Nm\ rad^2$
These stiffness and Damping values are inherent to the structure and depends only on the structural properties. Thus these values are called 'Structural Damping and Structural Stiffness'.

1.2.2 For the cases with airflow, $I_{EA}\ddot{\theta} + D_s\dot{\theta} + K_s\theta = M_{EA}$ calculate the system damped natural frequency (ω_d) and decay rates ($\xi\omega_n$) at different airspeeds, and plot theses values as a function of airspeed including the no-flow case. Calculate and plot the aeroelastic stiffness (Kae) and damping coefficients (Dae) as a function of airspeed as well.

Ans:

Apart from the free vibration case, an aerodynamic force is now being applied on to the system which effects the stiffness and damping itself. Combining the aerodynamic and structural properties gives us the Aeroelastic properties of the system. This aeroelastic stiffness and damping can also be found using the logarithmic decrement method as described previously.

From the graphs generated from Fig.1.13 to Fig.1.18, a damping ratio is selected (shown in red) followed by determining the damping and stiffness coefficients for all the cases with flow. A compiled table for the properties of wing for all the different flow is provided in Tab.1.1.

Variation of frequency and stiffness coefficient follows the same trend of quadratic decrease with air speed. This behaviour can also be seen from the steady aerodynamic model of symmetric wing with no initial angle of attack.

$$[K_s - e[\frac{1}{2}\rho U^2 cs(2\pi)]]\theta = 0 \tag{1.7}$$

Damping rate and damping coefficient rapidly increases with air speed.

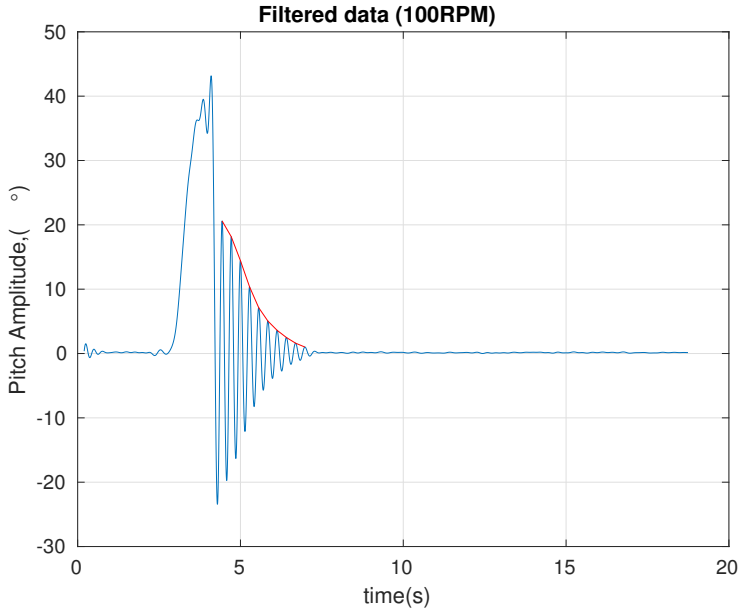

Figure 1.13: Filtered 100RPM Data

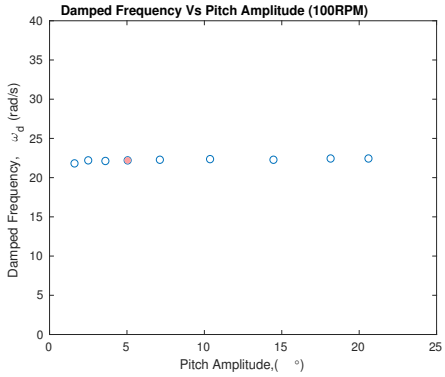

(a) Pitch Amplitude

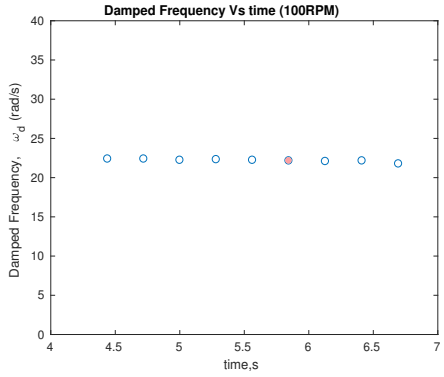

(b) Time

Figure 1.14: Variation of Damped Frequency

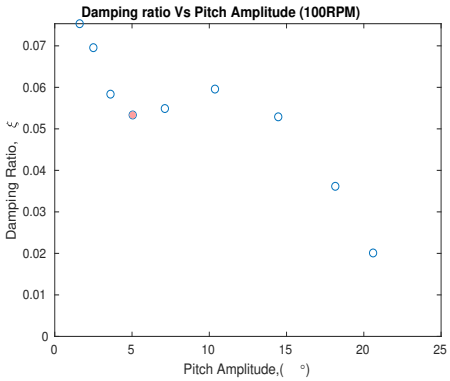

(a) Pitch Amplitude

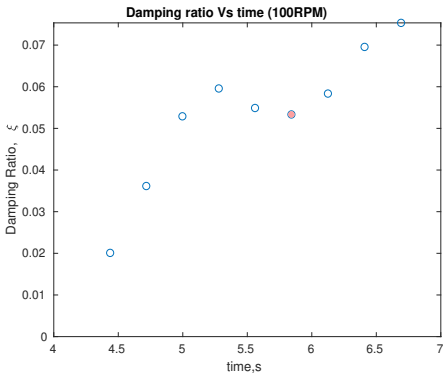

(b) Time

Figure 1.15: Variation of Damping Ratio

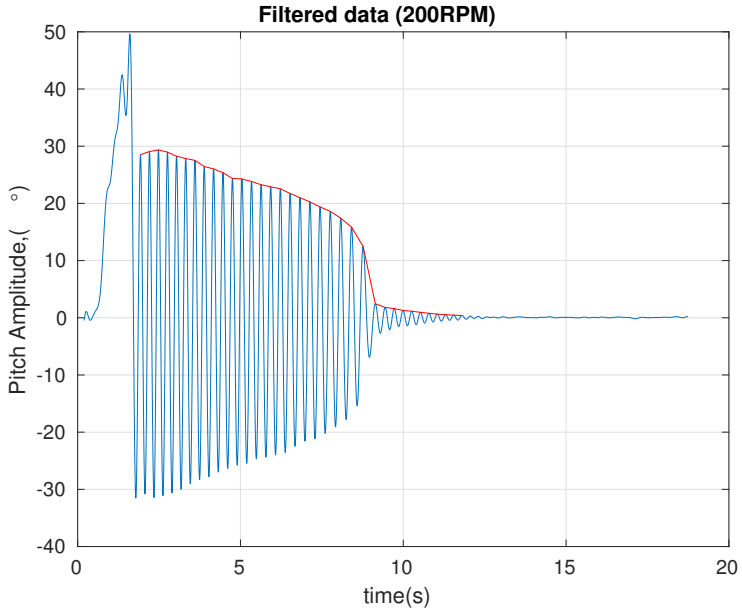

Figure 1.16: Filtered 200RPM Data

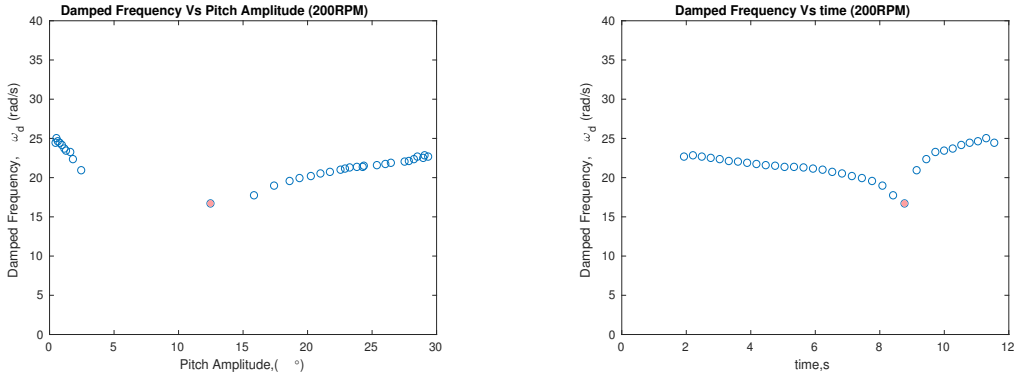

(a) Pitch Amplitude (b) Time

Figure 1.17: Variation of Damped Frequency

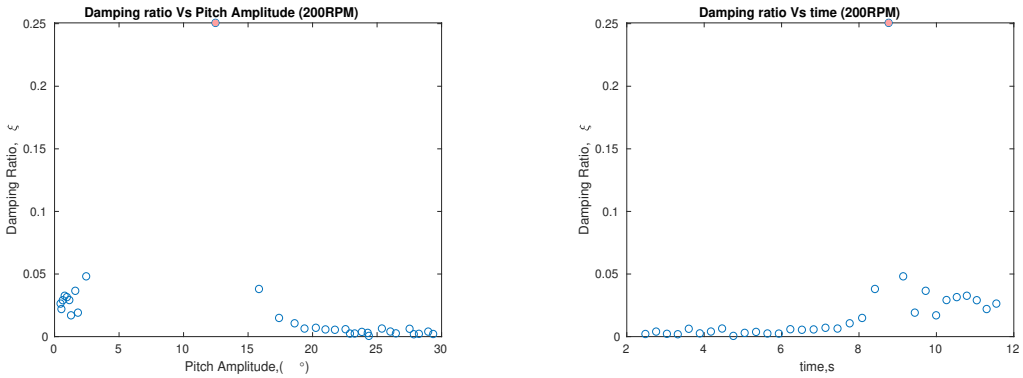

(a) Pitch Amplitude (b) Time

Figure 1.18: Variation of Damping Ratio

Table 1.1: Aeroelastic Properties of wing for different flow condition

Type of flow	**Free Vibration**	**100RPM**	**125RPM**	**150RPM**	**175RPM**	**200RPM**	**225RPM**
Air Speed U (m/s)	0	4.6	5.8	7	8.2	9.4	10.6
Damping Ratio ξ (%)	2.5	5.3	7.9	10.42	15.92	22.45	18.03
Time Period T (s)	0.264	0.283	0.291	0.313	0.349	0.398	0.409
Damped Natural Frequency ω_d (rad/s)	23.80	22.2	21.59	20.07	18	15.79	15.36
Natural Frequency ω_n (rad/s)	23.81	22.23	21.66	20.18	18.23	16.20	15.62
Damping Rate $\xi\omega_n$ (rad/s)	0.59	1.18	1.72	2.10	2.90	3.64	2.816
Damping Coefficient D_s $(Nm\ rad/s)$	0.0013	0.0026	0.0038	0.0046	0.0064	0.008	0.006
Stiffness Coefficient K_s $(Nm\ rad^2)$	0.624	0.548	0.516	0.448	0.366	0.289	0.268

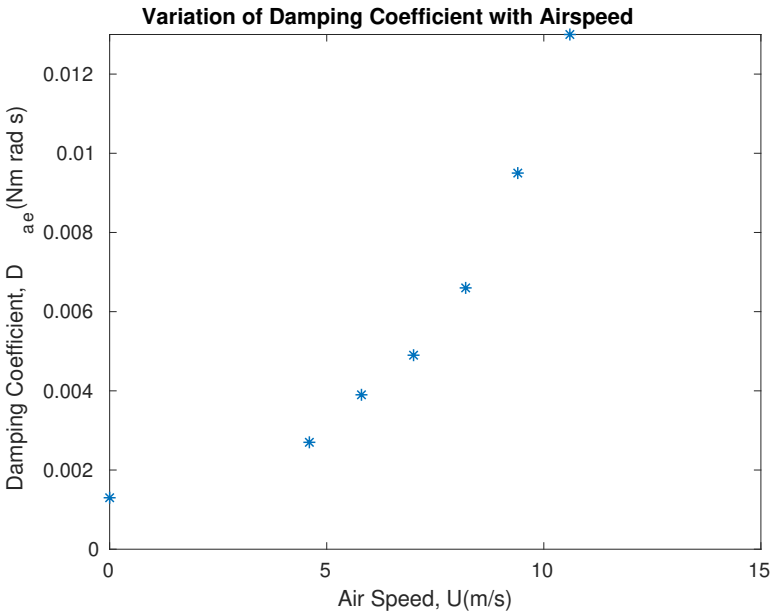

Figure 1.19: Variation of Damping coefficient with Air speed

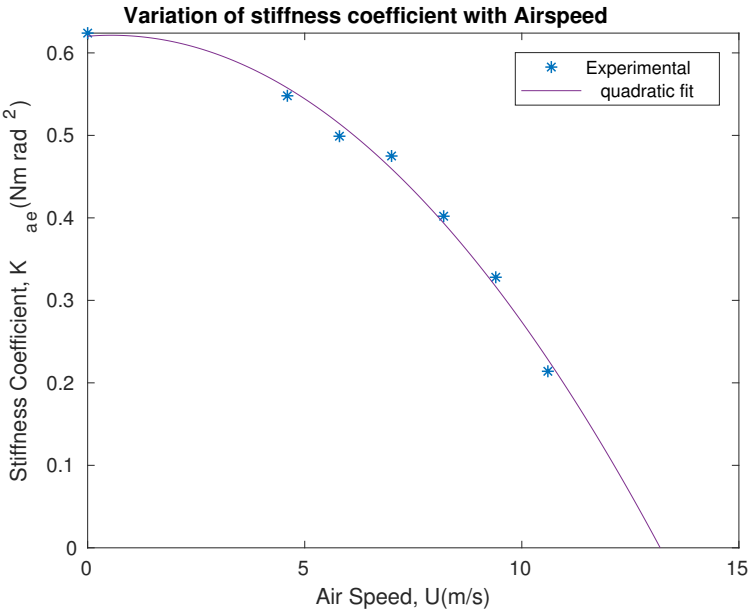

Figure 1.20: Variation of Stiffness Coefficient with Air Speed

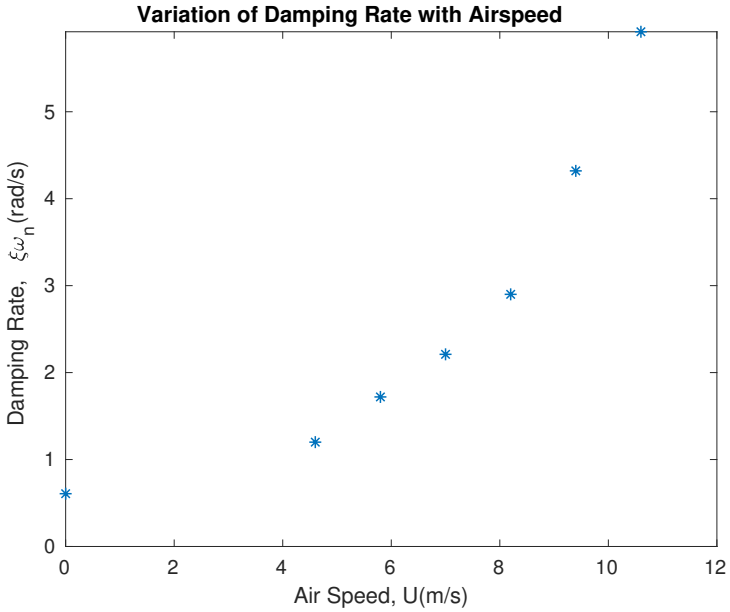

Figure 1.21: Variation of Damping Rate with Air Speed

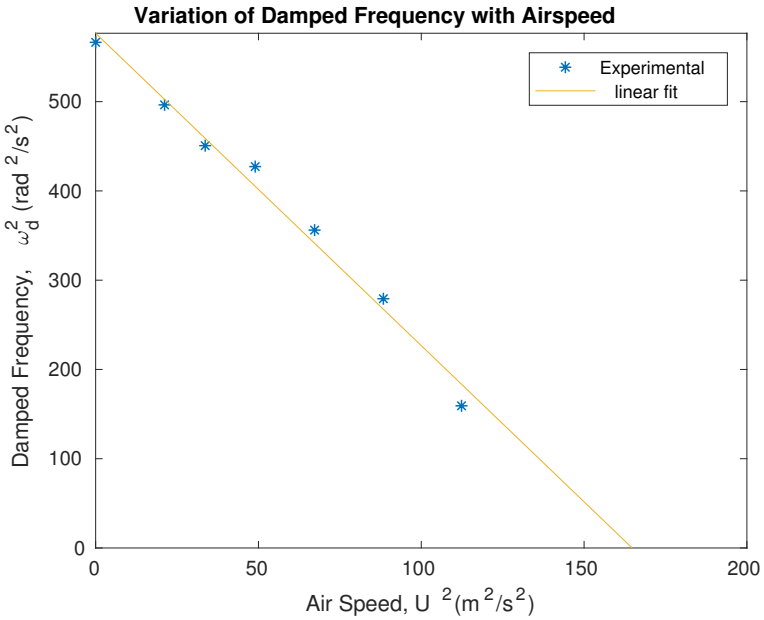

Figure 1.22: Variation of Damped Frequency with Air Speed

1.2.3 Compare the experimentally calculated frequencies and stiffness coefficients with those derived from an aeroelastic model using a steady aerodynamic model as seen in class.

From the aerodynamic equilibrium equation for steady aerodynamic case as in Eq. 1.7, substituting all the relevant values gives us the analytical stiffness coefficient for different flow rates. From Fig.1.23 and1.24 it can be seen that the steady aerodynamic model predicts the stiffness and divergence lower than the actual experimental results.

1.2.4 Compare the experimentally calculated aeroelastic stiffness and damping coefficients with those derived from an aeroelastic model using the following quasi-steady aerodynamic model

$$M_{EA} = e\frac{\rho U^2}{2}c(l)2\pi(\theta + \frac{\dot{h}}{U} + \frac{\dot{\theta}(3\frac{c}{4} - x_{EA})}{U}) - \frac{\rho U^2}{2}c^2(l)\frac{\pi c}{8U}\dot{\theta}. \tag{1.8}$$

Since the wing is allowed only pitching motion, heaving component in the equation is 0. Also, the stiffness coefficient part is same as the steady aerodynamic model and thus doesnt have any change from the previous calculated stiffness values. The aerodynamic damping part in the equation is added to the structural damping to get the aeoelastic damping,D_{ae}. A plot showing comparison of the experimental damping and the damping predicted by quasi steady equation is shown in Fig.1.25.

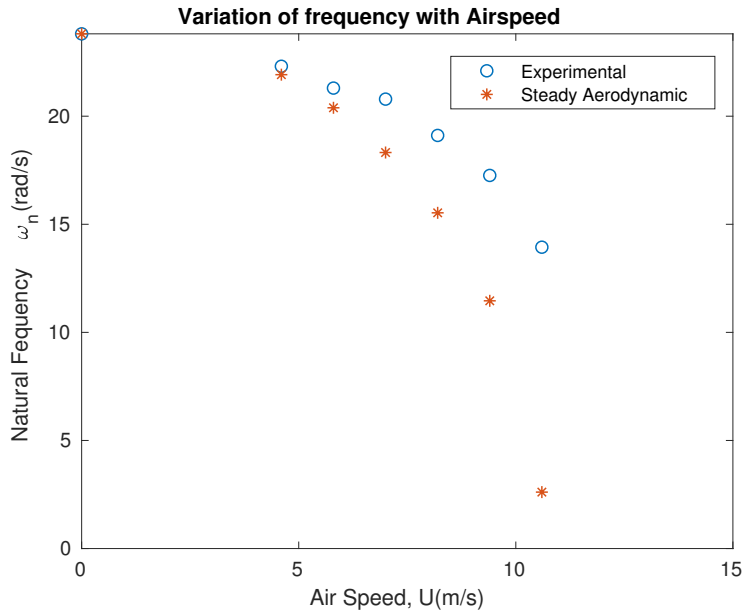

Figure 1.23: Variation of Frequency with Air Speed - Experimental and Steady Aerodynamic Model

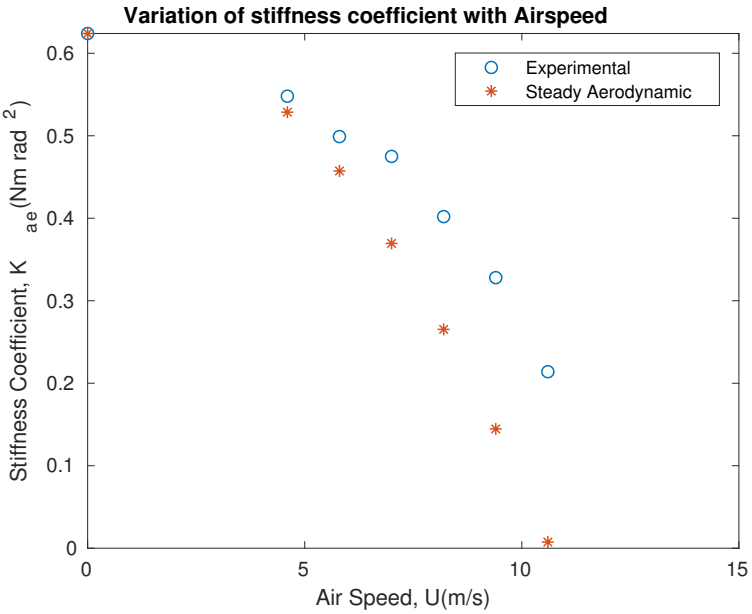

Figure 1.24: Variation of Stiffness Coefficient with Air Speed - Experimental and Steady Aerodynamic Model

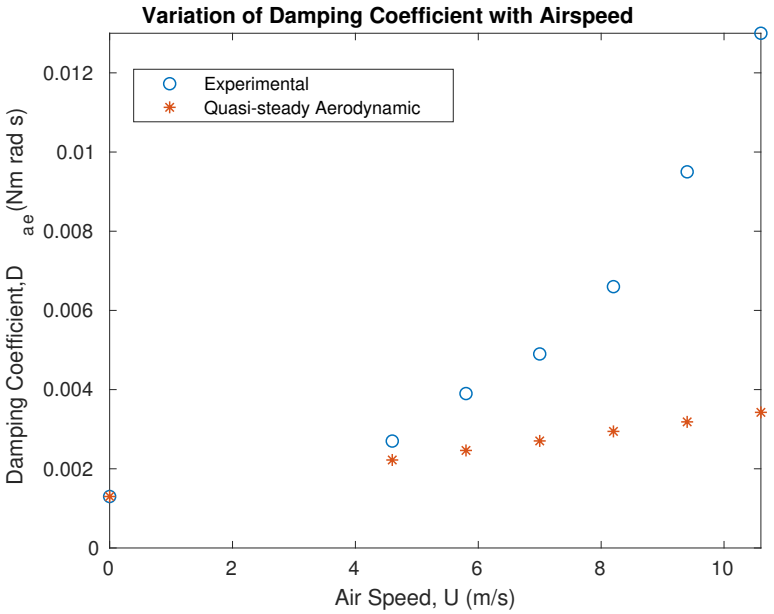

Figure 1.25: Variation of Damping Coefficient with Air Speed - Experimental and Quasi-Steady Aerodynamic Model

1.3 Divergence analysis

1.3.1 The divergence airspeed can be estimated by recalling that divergence occurs when the aeroelastic stiffness becomes zero. Realizing that Kae = Ks + Ka = Ks + AU2, where A is a constant, plot Kae as a function of U2 and extrapolate linearly to zero in order to obtain Udiv. Compare the value obtained with the theoretical divergence airspeed value.

Ans:

Plotting stifness coefficient (K_{ae}) as a function of U^2 gives us the divergence speed for which the line cuts x axis. Divergence occurs when the aeroelastic stiffness becomes 0. A plot showing the difference of divergence air speed for steady aerodynamic model and the experimental results is shown in Fig.1.26. Divergence air speed found from the plot are :

Experimental
$U_{div}{}^2 = 177.9m^2/s^2$
$U_{div} = 13.33m/s$

Theoretical
$U = 10.60m/s$

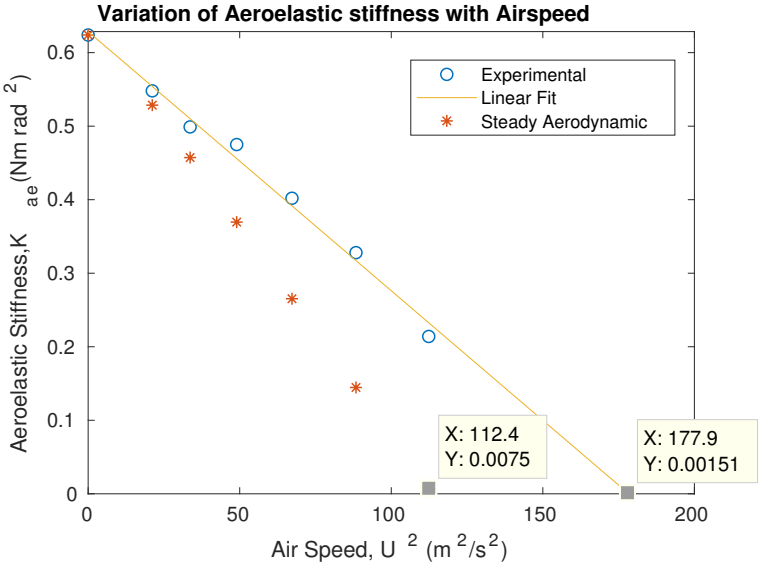

Figure 1.26: Divergence Air Speed- Experimental and Steady State Model

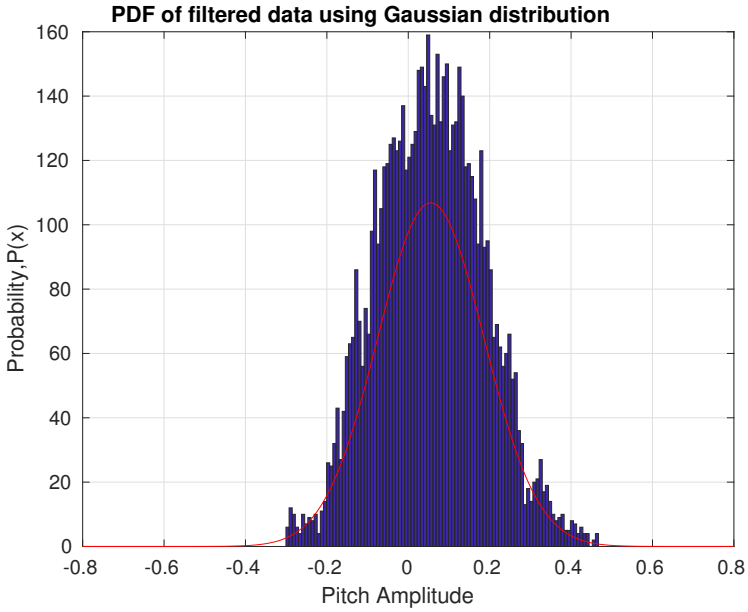

Figure 1.27: Variation of Equilibrium Pitch with Airspeed

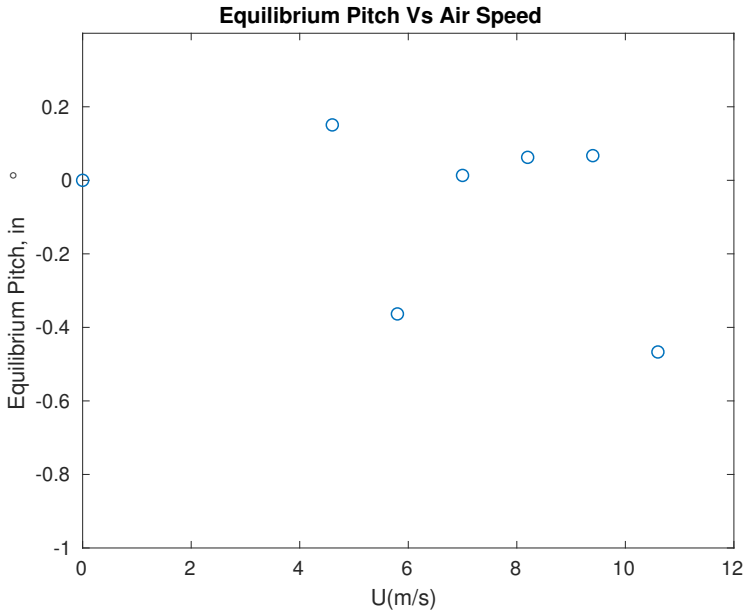

Figure 1.28: Variation of Equilibrium Pitch with Airspeed

1.3.2 Plot the position of the equilibrium point as a function of airspeed. What happens when you get close to divergence?

Equilibrium point is the state at which the wing settles down after oscillation. To find out the correct representative equilibrium point, generate a PDF of the signal from a part after the oscillations to end of time. The mean of the PDF matching with a Gaussian distribution can be taken as the equilibrium point for that flow (Fig. 1.27). A plot showing the variation of equilibrium pitch for various flows have been shown in Fig.1.28. The equilibrium pitch varies from '0' value throughout the flow rates which suggests that the aerofoil has a bias. Since aerofoil is placed vertically and doesn't have any camber, the bias must be because of initial angle of attack. As we move closer to the divergence speed the equilibrium pitch increases as expected.

1.3.3 Based on the equation seen in class with a bias, and the test results, estimate the magnitude of the initial angle of attack, α_0, if any

From euqation for equilibrium pitch angle, Eq.1.9 substituting for the air speed and equilibrium pitch angle gives us the bias.

$$\theta_{eq} = \frac{e[\frac{1}{2}\rho U^2 cs(2\pi)]\alpha_0}{K - e[\frac{1}{2}\rho U^2 cs(2\pi)]} \tag{1.9}$$

When calculated with $U = 5.8m/s$, and $eq = -0.3634\,\text{deg}$ initial angle of attack $0 = -0.82\,\text{deg}$. Since the variation in equilibrium pitch is not showing any particular trend, its difficult to predict that the bias is from angle of attack. These variations could be due to other errors in the experimental setup too.

1.4 Summary

Noise Properties Analysis

* Noise in the signal effects and changes its inherent properties extensively and thus requires careful examination.

* Filtering out the proper amount of noise from the signal, deciding the cutoff and pass band frequencies, has huge impact on the further analysis.

* Probability Spectral Density Function (PSDF) tells us the distribution of frequencies in the signal and the major contributing ones among them.

* Cutoff and passband can be decided based on finding out how well the noise can be approximated to a particular distribution (PDF) where we can represent it by its mean and variance.

* Histogram plots are also of easy visualisation technique to understand the distribution of data before and after filtering, which confirms any major loss of data.

* The mean of this noise has to be accounted while converting the unit of measurement to desired units of analysis.

Aeroelastic Analysis

* Filtering out the noise considering its properties found in the previous analysis has to be done correctly before any analysis with the data is made. This has to be done considering to capture the inherent frequency present in the signal and to get smooth and clear peak values.

* Logarithmic decrement method can be easily applied to find out the damping ratio, damping rate , natural and damped frequency, stiffness and damping coefficients.

* In the case of a wing subjected to airflow, since it is likely to have non-linearities due to stall and Reynolds number effects one should take only the peaks in the linear regime for accurate results.

* Linear cycles can be estimated by examining the variation of damping ratio and damped frequency with pitch amplitude and time.

* Damping rate and Damping coefficient shows the same trend with increase in air speed. Both values increase parabolically with airspeed.

* Damped frequency and stiffness coefficient also show the same trend with increase in airspeed. Both values decrease when approaching higher speeds.

* Comparison of stiffness coefficient and frequency of experimental and steady aerodynamic model shows interesting results. Experimental results for stiffness are higher than the analytical model at different airspeeds till divergence.

* Both values are comparable at lower air speeds but with increase in U, they differ greatly which tend to 0 as U approaches divergence speed.

* Comparison of damping coefficient to a quasi steady model shows that the experimental values are higher than the linearly varying quasi steady model.

Divergence Analysis

* Divergence speed in the experimental case is higher than the analytical one as expected from the difference in stiffness coefficients seen.

* While experimental results give 13.33 m/s analytical model shows a divergence speed of 10.66 m/s.

* Equilibrium pitch angle is very low and is near to 0 value. As expected the values tend to slightly increase as we move closer to divergence speed. There is no particular trend in the variation of equilibrium pitch and thus its difficult to predict any bias. However, as a sample calculation, initial angle of attack found with an airspeed of U = 5.8 m/s is -0.82 degree.

Chapter 2

Divergence of 3D Wing

2.1 Analytical Solution for a 3D Wing

As per the wing data given for NACA 2412, it has a maximum camber of 2% at 40% chord length and a maximum total thickness of 12% chord length. For locating the Elastic axis of the wing, one need to find the flexural center of the structure. In this case flexural center can be found for a system with an I section with unequal flanges. From AIAA Aerospace Design Engineers Guide, eccentricity from the centroid of first flange to the flexural center of an I section with length b between the flanges is given as in Eq.2.1.

$$e = b\left(\frac{I_2}{I_1 + I_2}\right) \tag{2.1}$$

e value is found to be $0.1105c$ from the first spar and $0.3605c$ from leading edge. Assuming a subsonic flow aerodynamic center is located at $0.25c(c/4)$. Thus eccentricity between AC and EA can be calculated as $0.1105c$. Also, for the wing which is assumed to be in the trapezoidal shape, variation of chord along the span can be found as

$$c(y) = 2 \times \left[0.6(1 - \frac{y}{s}) + 0.4\right] \tag{2.2}$$

Assuming strip theory aerodynamics, total aerodynamic moment about elastic axis for a thin strip of dy at length y distance from root in a 3D wing can be written as below.

$$dM_{EA} = edL + dM_{AC} \tag{2.3}$$

$$dM_{EA} = \frac{\rho U^2}{2}[e(y)c(y)C_{L_\alpha}(y)(\theta + \alpha_0) + c^2(y)C_{m_{AC}}(y)]dy \tag{2.4}$$

where $C_{l\alpha}$ and C_{MAC} are

$$C_{L_\alpha}(y) = 2\pi\left[\sqrt{1 - \left(\frac{y}{s}\right)^2}\right] \tag{2.5}$$

$$C_{m_{AC}}(y) = 0.05\left[\sqrt{1-\left(\frac{y}{s}\right)^2}\right] \tag{2.6}$$

$$U_{div}(y) = \frac{1}{2s}\left[\sqrt{\frac{180\times GJ(y)}{\rho ec\sqrt{1-\left(\frac{y}{s}\right)^2}}}\right] \tag{2.7}$$

2.2 Assumed Mode Method

2.2.1 Suppose the following assumed mode representation: $\theta = \sum_{i=1}^{n} \bar{\theta}_i \eta^i$ Calculate the divergence airspeed for as many modes that are needed to obtain convergence on the calculated divergence airspeed

For polynomial assumed modes, E structural stiffness matrix and the $\bar{K}$ aerodynamic stiffness matrix can be found from the lagrange's equation as(Ref. Slides-AE503)

$$E_{ij} = \frac{1}{s}\int_0^1 GJ(\eta) f'_i f'_j d\eta \tag{2.8}$$

$$\bar{K}_{ij} = s\int_0^1 e(\eta)c(\eta)C_{L_\alpha}(\eta) f_i f_j \tag{2.9}$$

$$F_i = s\frac{\rho U^2}{2}\left[\int_0^1 (e(\eta)c(\eta)C_{L_\alpha}(\eta) f_i \alpha_0 d\eta + c^2 C_{m_{AC}} f_i) d\eta\right] \tag{2.10}$$

where, $\eta = \frac{y}{s}$ and f_i, f_j are the polynomial modes α_0 is the geometric twist and $GJ(\eta)(Nm^2/\deg)$

$$GJ(\eta) = 20000\left[1-\left(\frac{\eta}{1.5}\right)^4\right]^{0.5} \tag{2.11}$$

For divergence to occur, it can be established that the determinant of sum of E and $K(-\bar{K})$ should be 0. This could be considered as an eigen value problem as

$$\lambda = eig(E, \frac{\bar{K}}{q}) \tag{2.12}$$

where λ's and q are the dynamic pressure. Divergence air speed can be calculated from the eigen values as

$$U_{div} = \sqrt{\frac{2\lambda}{\rho}} \tag{2.13}$$

Using the polynomial modes as per the question, the converged divergence airspeed is

$U_{div} = 246.96\ m/s$.

2.2.2 Instead of the polynomial modal representation, suppose that the assumed modes are the normal modes for a uniform cantilevered beam in torsion (for instance Hodges and Pierce, 2002). Do the same as question 1 and compare both sets of results.

As per Hodges and Pierce,2002 the normal modes for a cantilever beam in torsion is written as

$$f_i(y) = \sin\left(\frac{(2i-1)\pi y}{2s}\right) \tag{2.14}$$

Using this modal representation for calculating the eigen values and divergence from that,

$U_{div} = 246.96\ m/s$. While the polynomial modal representaion converged with 5 modes the torsional modes converged with just 3 modes to the exact same value. This clearly explains that the divergence of a wing essentially a cantilever beam fixed at the root, is more realistically represented by the torsional modes of the cantilever beam.

Table 2.1: Divergence of 3D Wing(m/s)- Assumed Mode Method

Number of Modes	1	2	3	4	5	6
Polynomial Mode	303.41	247.83	247.41	247	246.96	246.96
Torsional Mode	254.43	246.99	246.97	246.96	246.96	246.96

2.2.3 Do you think you need to correct for compressibility effects?

Mach number for the given problem as per the divergence air speed calculated above can be found as,

$$M_\infty = \frac{U_{div}}{c} = 0.72 \tag{2.15}$$

where, c is the speed of sound in air $343\ m/s$. When the value of mach number exceeds 0.3 and less than 0.8 the flow remains subsonic but the air is compressible. This means that the lift curve slope should be corrected. Prandtl-Glauert correction for lift coefficient can be used here as,

$$C_{L_\alpha} = \frac{\bar{C}_{L_\alpha}}{\sqrt{1 - {M_\infty}^2}} \tag{2.16}$$

This correction while applied changes C_{L_α} in turn changes the $\bar{K}$ matrix and the divergence air speed. Thus, solving iteratively for the convergence of mach number, a corrected divergence speed can be obtained. This value is obtained as

$U_{div,corrected} = 217.30\ m/s.$

2.2.4 By calculating the system parameters at different spanwise locations (say at 10different locations), apply the analytical solution and obtain 10 estimates of the divergence airspeed by assuming that the wing properties are given by the local properties at each location. Do not forget that the lift curve slope is a function of y.Which wing station gives the best estimate when compared with the assumed mode solution?

By taking 10 discrete points along the sapn and considering the local values of each variables divergence speed can be estimated as per Eq.2.7. Since at the tip of the wing, C_{L_α} goes to 0 the divergence speed jumps to infinity. By looking at the fig.2.1, one can see that the divergence speed increases from the root of the wing to tip parabolically. From the previous estimate of divergence speed 246.96 m/s, the location in the span which gives same divergence speed is found from interpolation as 6.64 m.

Table 2.2: Divergence of 3D Wing along Span(m/s)- Analytical

Location along Span,y(m)	1	2	3	4	5	6	7	8	9	10
Divergence Speed,$U(m/s)$	137.50	147.99	160.91	176.97	197.30	223.76	259.86	313.40	410.03	inf

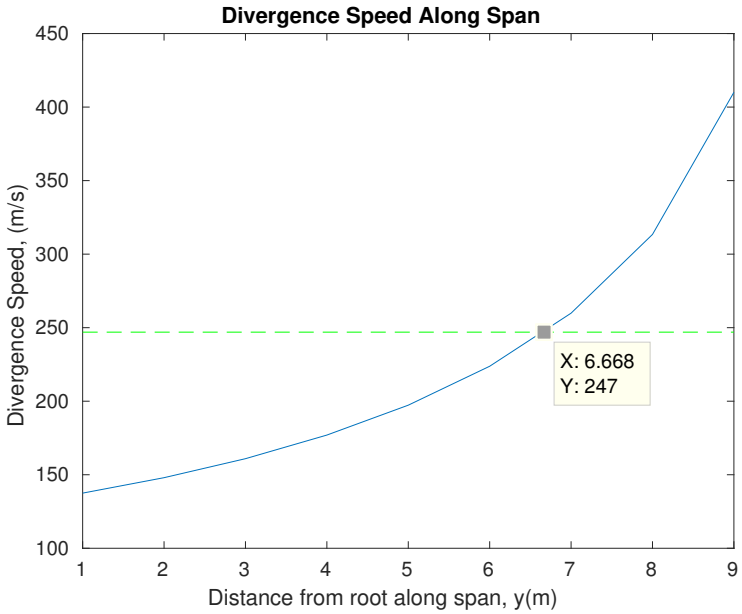

Figure 2.1: Divergence Air Speed along Span-Analytical

2.2.5 For a pre-divergence airspeed of your choice, calculate and plot the aeroelastic twist distribution, $\theta(y)$, along the wing span for the one-mode, two-mode and three-mode models.

Twist distribution along span can be found for the assumed mode method by the following equations. For a given air speed,U less than the divergence speed $\bar{\theta}$ is found as,

$$\{\bar{\theta}\} = \left[[E] - [\bar{K}]\right]^{-1} \{F\} \tag{2.17}$$

where matrices $[E], [\bar{K}], F$ are as described in section 2.2. From $\bar{\theta}$, $\theta(y)$ can be found from the assumed mode equation as in 2.2. Twist distribution plotted for 3 modes in polynomial and torsional modal representation is shown in figures below (Fig.2.2, Fig.2.3). It can also be seen that the torsional modes clearly captures the behavior of the wing more rapidly and efficiently than polynomial modes.

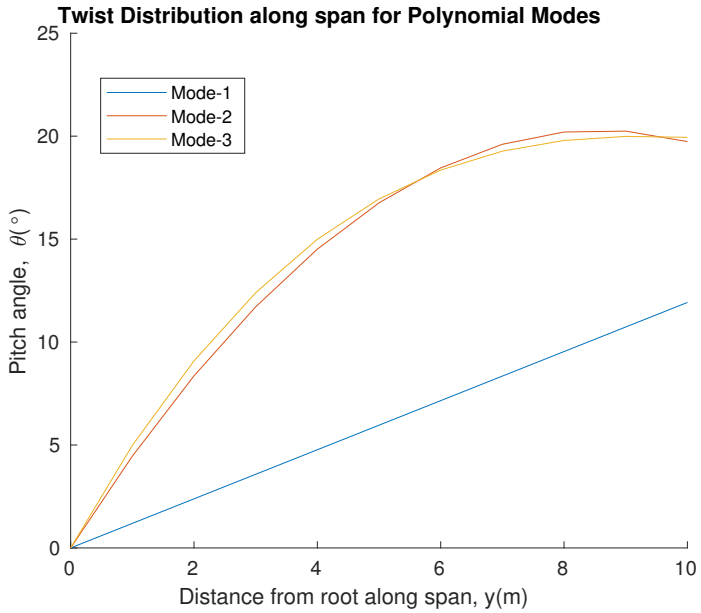

Figure 2.2: Twist Distribution along span- Polynomial Modes

2.3 Summary

Divergence of 3D Wing-Assumed Mode Method

* Different from a 2D aerofoil analysis of 3D wing requires consideration of 3D effects, which effects the lift and moment coefficient slopes.
* Assumed mode method can be suitably used for easy calculation of divergence air speed.
* Polynomial modal representation requires more number of modes to capture the divergence speed than the torsional modes which converges faster. Torsional modes of a cantilever can be seen as a more realistic representation of the wing which also behaves as a cantilever in torsion for pitch rotations.

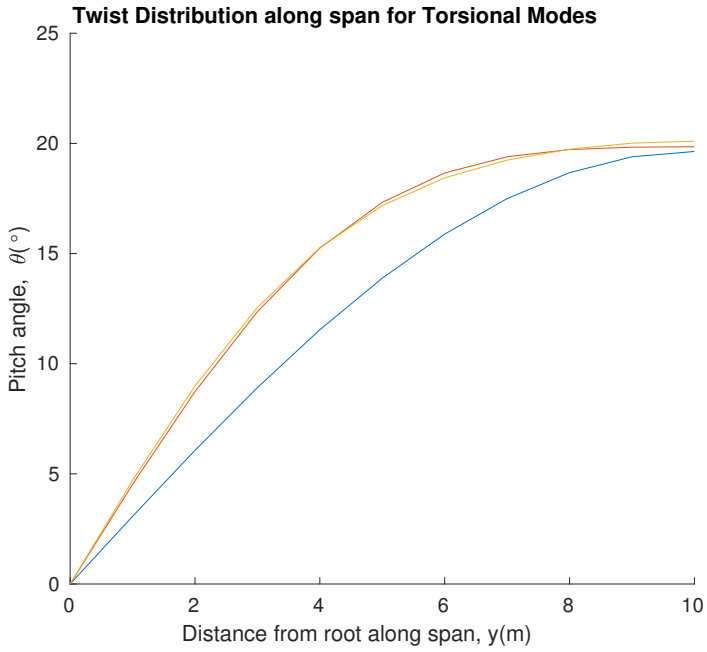

Figure 2.3: Twist Distribution along span- Torsional Modes

* Divergence speed calculation at local points along the span shows that 6.64 m from root shows the same value as calculated from assumed mode method.

* Since the mach number is more than 0.3, compressibility of the medium should also be considered for the analysis. This effects the lift coefficient which can be modified using the Prandtl-Glauert equations. Iterating over this correction to calculate new divergence speed and mach number till convergence gives a value of 217.30 m/s.

* Twist distribution along the sapn for the wing can also be obtained from assumed mode method which shows the pitch angle at various locations for different modes.

Chapter 3

Coupled Flutter Analysis

Equation of motion in pitch and heave for coupled flutter can be seen as

$$I_\theta \ddot{\theta} + \frac{M_\theta c x_\theta}{2} \ddot{h} + D_\theta \dot{\theta} + K_\theta \theta = M_{EA} \tag{3.1a}$$

$$M_h \ddot{h} + \frac{M_\theta c x_\theta}{2} \ddot{\theta} + D_\theta \dot{h} + K_h h = -L \tag{3.1b}$$

where, lift L and moment about elastic axis $M_E A$ are expressed combining unsteady aerodynamic circulatory terms from Wagner and non-circulatory terms from Theodorsen as,

$$L = b^2 s\rho\pi \left[\ddot{h} + U\dot{\theta} - ba_h\ddot{\theta}\right] + \rho U b s 2\pi \left[(1 - A_1 - A_2)\, w_{\frac{3c}{4}}(t) + \dot{z}(t)\,(A_1 b_1 + A_2 b_2) + z(t) b_1 b_2\,(A_1 + A_2)\right] \tag{3.2}$$

$$\begin{aligned} M_{EA} = {} & b^2 s\rho\pi \left[b a_h \ddot{h} - Ub(0.5 - a_h)\dot{\theta} - b^2(1/8 + {a_h}^2)\ddot{\theta}\right] \\ & + \rho U b^2 s 2\pi (a_h + 0.5) \left[(1 - A_1 - A_2)\, w_{\frac{3c}{4}}(t) + \dot{z}(t)\,(A_1 b_1 + A_2 b_2) + z(t) b_1 b_2\,(A_1 + A_2)\right] \end{aligned} \tag{3.3}$$

$$\ddot{z} + \dot{z}(t)\,(b_1 + b_2) + z(t) b_1 b_2 = w_{\frac{3c}{4}}(t) \tag{3.4}$$

where,

$$w_{\frac{3c}{4}}(t) = U\theta + \dot{h} + \dot{\theta} b(0.5 - a_h) \tag{3.5}$$

$$A_1 = 0.165, A_2 = 0.335, b_1 = 0.0455\frac{U}{b}, b_2 = 0.3\frac{U}{b} \tag{3.6}$$

3.0.1 Assuming unsteady aerodynamics with Wagners circulatory two lag terms representation and Theodorsen's non-circultory terms,express the system of equation in matrix form and identify the coupling terms. Do not forget to consider the span when writing the aerodynamic terms

Substituting expression for lift and moment in Eq.3.1b and 3.1a respectively gives us,

$$\left[M_h + b^2 s\rho\pi\right]\ddot{h} + \left[\frac{M_\theta c x_\theta}{2} - (b^2 s\rho\pi(ba_h))\right]\ddot{\theta} + \left[D_h + \rho U b s 2\pi\left(1 - A_1 - A_2\right)\right]\dot{h} + K_h h + \left[b^2 s\rho\pi U + \rho U b s 2\pi\left(1 - A_1 - A_2\right) b(0.5 - a_h)\right]\dot{\theta} + \left[\rho U b s 2\pi\left(1 - A_1 - A_2\right) U\right]\theta + \left[\rho U b s 2\pi\left(A_1 b_1 + A_2 b_2\right)\right]\dot{z}(t) + \left[\rho U b s 2\pi b_1 b_2\left(A_1 + A_2\right)\right] z(t) = 0 \quad (3.7)$$

$$\left[I_\theta + b^2 s\rho\pi \times b^2(1/8 + {a_h}^2)\right]\ddot{\theta} + \left[\frac{M_\theta c x_\theta}{2} - (b^2 s\rho\pi(ba_h))\right]\ddot{h} + \left[D_\theta + b^2 s\rho\pi \times U b(0.5 - a_h) - (\rho U b^2 s 2\pi(a_h + 0.5)\left(1 - A_1 - A_2\right) b(0.5 - a_h)\right]\dot{\theta} + \left[K_\theta - (\rho U b^2 s 2\pi(a_h + 0.5)\left(1 - A_1 - A_2\right) U)\right]\theta - \left[\rho U b^2 s 2\pi(a_h + 0.5)\left(1 - A_1 - A_2\right)\right]\dot{h} - \left[\rho U b^2 s 2\pi(a_h + 0.5)\left(A_1 b_1 + A_2 b_2\right)\right]\dot{z}(t) + \left[\rho U b^2 s 2\pi(a_h + 0.5) b_1 b_2\left(A_1 + A_2\right)\right] z(t) = 0 \quad (3.8)$$

$$\ddot{z} + \dot{z}(t)\left(b_1 + b_2\right) + z(t) b_1 b_2 - U\theta - \dot{h} - \dot{\theta} b(0.5 - a_h) = 0 \quad (3.9)$$

$$[M]\begin{Bmatrix}\ddot{h}\\ \ddot{\theta}\\ \ddot{z}\end{Bmatrix} + [C]\begin{Bmatrix}\dot{h}\\ \dot{\theta}\\ \dot{z}\end{Bmatrix} + [K]\begin{Bmatrix}h\\ \theta\\ z\end{Bmatrix} = \begin{Bmatrix}0\\ 0\\ 0\end{Bmatrix} \quad (3.10)$$

where,

$$[M]\begin{Bmatrix}\ddot{h}\\ \ddot{\theta}\\ \ddot{z}\end{Bmatrix} = \begin{bmatrix} M_h + b^2 s\rho\pi & \frac{M_\theta c x_\theta}{2} - (b^2 s\rho\pi(ba_h)) & 0 \\ \frac{M_\theta c x_\theta}{2} - (b^2 s\rho\pi(ba_h)) & I_\theta + b^2 s\rho\pi \times b^2(1/8 + {a_h}^2) & 0 \\ 0 & 0 & 1 \end{bmatrix}\begin{Bmatrix}\ddot{h}\\ \ddot{\theta}\\ \ddot{z}\end{Bmatrix} \quad (3.11)$$

$$[C]\begin{Bmatrix}\dot{h}\\ \dot{\theta}\\ \dot{z}\end{Bmatrix} = \begin{bmatrix} D_h + \rho U b s 2\pi\left(1 - A_1 - A_2\right) & b^2 s\rho\pi U + \rho U b s 2\pi\left(1 - A_1 - A_2\right) b(0.5 - a_h) & \rho U b s 2\pi\left(A_1 b_1 + A_2 b_2\right) \\ -\rho U b^2 s 2\pi(a_h + 0.5)\left(1 - A_1 - A_2\right) & D_\theta + b^2 s\rho\pi \times U b(0.5 - a_h) - (\rho U b^2 s 2\pi(a_h + 0.5)\left(1 - A_1 - A_2\right) b(0.5 - a_h) & -\rho U b^2 s 2\pi(a_h + 0.5)\left(A_1 b_1 + A_2 b_2\right) \\ -1 & -b(0.5 - a_h) & (b_1 + b_2) \end{bmatrix}\begin{Bmatrix}\dot{h}\\ \dot{\theta}\\ \dot{z}\end{Bmatrix} \quad (3.12)$$

$$[K]\begin{Bmatrix} h \\ \theta \\ z \end{Bmatrix} = \begin{bmatrix} K_h & \rho U^2 bs2\pi\left(1-A_1-A_2\right) & \rho Ubs2\pi b_1 b_2\left(A_1+A_2\right) \\ 0 & K_\theta - \left(\rho U^2 b^2 s2\pi(a_h+0.5)\left(1-A_1-A_2\right)\right) & -\rho Ub^2 s2\pi(a_h+0.5)b_1 b_2\left(A_1+A_2\right) \\ 0 & -U & b_1 b_2 \end{bmatrix}\begin{Bmatrix} h \\ \theta \\ z \end{Bmatrix} \tag{3.13}$$

From the matrices M, C and K we can see that the coupling terms are $M_{12}, M_{21}, C_{12}, C_{21}$ and K_{12}.

Converting to Laplace domain and rewriting equation gives us,

$$\begin{bmatrix} \mathrm{H} \\ \Theta \\ \mathrm{Z} \end{bmatrix} = \left[s^2\left[M\right]+s\left[C\right]+\left[K\right]\right]^{-1}\left\{IC(s)\right\} = \left[A(s)\right]^{-1}\left\{IC(s)\right\} \tag{3.14}$$

3.0.2 Calculate the flutter speed by calculating the roots (i.e. the eigenvalues) of the characteristic equation as you sweep in airspeed. You can also obtain the eigenvalues by expressing the aeroelastic system in state-space form.

For finding out the roots which leads to flutter, determinant of $[A(s)]$ should be zero. Solving this polynomial of 6 degree gives us 6 roots which contains two complex conjugate roots of the form $\beta + i\omega_d$, where β is the decay rate and ω_d is the coupled frequency. For identifying the correct decay rate and frequency of the solution one has to also note that the Z roots are real and have 0 imaginary part. While, sweeping through the air speed one may also encounter divergence air speed where one of the frequency (Pitch Dominated Mode) reduces to zero. So, its better to identify the divergence air speed and then sweep through the values before this speed. Divergence speed can be estimated from modifying the equation of motion (removing the dynamic terms) for pitch degree of freedom as,

$$K_\theta \theta = M_{EA} \tag{3.15}$$

where, M_{EA} is as specified in Eq.3.3 removing all the un-ncessary dynamic terms.

$$U^2 = \frac{K_\theta}{\rho b^2 s2\pi(a_h+0.5)\left(1-A_1-A_2\right)} \tag{3.16}$$

Sweeping through the air speed one can calculate the roots of the equation. The point at which the decay rate reduces to 0 or changes its sign is considered as flutter point and is calculated as 9.3 m/s.

3.0.3 Plot the eigenvalues (remember they have two parts) of the system as the airspeed is swept (increased) from zero to some post-flutter value; ie the V-f and $V-\beta$ diagram. Report and explain any observations; amongst other things identify which mode is which

All the roots of the polynomial are plotted in Fig.3.1 with varying air speed. Since Z values are of not any interest at this point, variation of frequency and decay rate are seperated out from this plot.

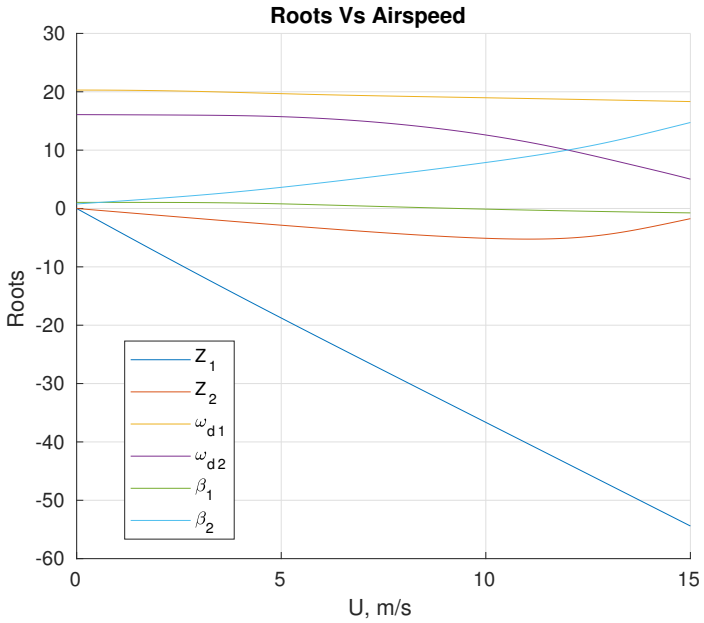

Figure 3.1: Variation of Roots of Polynomial with Airspeed

With respect to the closeness of coupled frequency to uncoupled frquency at 0 air speed, one can distinguish the modes to be heave dominated or pitch dominated. They can also be identified by looking at the eigen vectors which gives a ratio of displacement. With increasing air speed the modes can no longer be clearly distingusihed and may move closer or away from uncoupled frequencies. Variation of decay rate, β is plotted with air speed up to a post flutter value in Fig.3.2. In the present case, while the pitch dominated mode decay rate increases with air speed, the heave dominated mode is decreasing. The point at which this mode crosses the 0-axis is considered as the flutter line. Variation of frequency for the two modes are also plotted in Fig.3.3. Uncoupled frequecies of pitch and heave are found to be 16.51 rad/s and 20 rad/s respectively. The coupled frequencies can be seen to be closely following the uncoupled frequencies at first but decreasing from it as we sweep through the air speed. The pitch mode frequency can be seen to be dropping to zero value as we increase air speed which is due to divergence of wing. The flutter speed frequencies are found to be 13.29 rad/s and 19.06 rad/s for pitch and heave dominated modes respectively. But it can be noted that the pitch frequency dies out really quick because of the increasing decay rate as can be seen from the previous figure. So, the flutter frequency can be estimated to be only the heave dominated frequency which is 19.06.

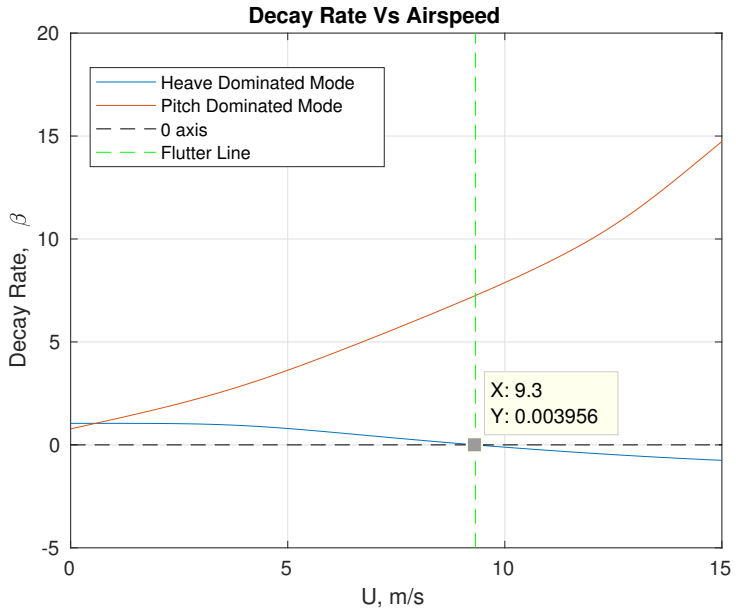

Figure 3.2: Variation of Decay Rate, β with Airspeed

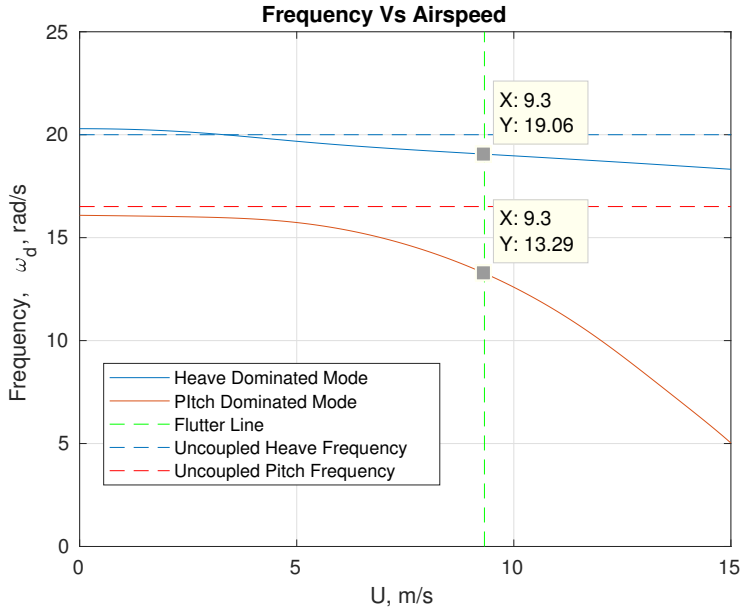

Figure 3.3: Variation of Coupled Frequency, ω_d with Airspeed

3.0.4 By changing the value of the heave structural stiffness coefficient, modify the frequency ratio $\frac{\omega_h}{\omega_\theta}$ from its original value and observe how the flutter speed varies with the frequency ratio. Expect a similar plot as seen in class. Report and explain any observations.

By varying the structure stiffness coefficient, K_h one can obtain different ω_h values and correspondingly different frequency ratio $\frac{\omega_h}{\omega_\theta}$ values. A plot of the variation of this frequency ratio with corresponding flutter speed values is plotted in fig.3.4. The graph provides us with really significant and interesting results related to flutter.

* The stiffness coefficient of the wing is the most important quantity which dictates the flutter air speed for the wing.

* Varying K_h or K_θ can reduce or increase the flutter speed and can cause fatal damage if not properly accounted for.

* One can partition the graph in to two safe zones, one with a frequency ratio more than 0.9 and one with a value less than 0.9.

* As for the present case with flutter speed of 9.3 m/s, one can only increase the heave structural stiffness coefficient which will increase the frequency ratio. But instead, if one choses to increase the pitch stiffness, the frequency ratio decreses which will reduce the flutter speed thus contributing to the contrary.

3.1 Summary

Coupled Flutter

* Coupled Flutter phenomenon is more complex and significant for aircraft wings than divergence, especially since it occurs at a lower air speed.

* Mass and Damping terms play an important role in coupled flutter while the flutter speed is dictated by the frequency or the stiffness of wing.

* It is really important to plot the frequency ratio variation with flutter speed before increasing or decreasing any of the structural stiffness values since it directly affects the flutter.

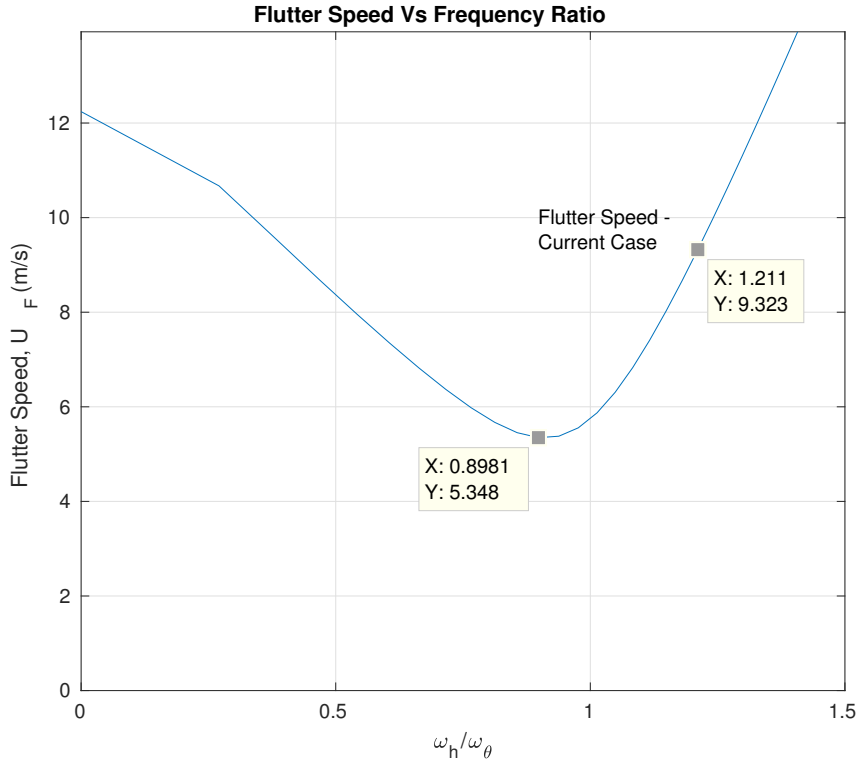

Figure 3.4: Variation of Frequency Ratio, $\frac{\omega_h}{\omega_\theta}$ with Flutter Speed